American Mineralogist, Volume 60, pages 815–823, 1975

Oxygen Fugacity Values of Furnace Gas Mixtures[1]

J. Stephen Huebner

Stop 959, U.S. Geological Survey, Reston, Virginia 22092

Abstract

Comparison of oxygen fugacity values measured electrochemically with values calculated thermochemically from the gas-mixing ratio indicates that gas equilibrium is not always obtained within a furnace. The prevailing oxygen fugacity value actually depends upon at least five factors that are controlled by the experimentalist: initial gas composition, temperature, flow rate, hot-spot configuration, and position of sensor or sample. As a general rule, CO_2-H_2 mixtures reach a steady state or equilibrium by the time they are heated to 1125°-1225°C; for CO_2-CO mixtures, the temperature range is 1050°-1150°C. At temperatures greater than these minimum values, oxygen fugacities can be maintained and measured with a precision of ±0.02 and an accuracy better than ±0.1 log atm units.

Introduction

Recent investigations of crystal-liquid equilibria of iron-bearing silicate systems have emphasized the difficulties of maintaining sample bulk composition. Interaction of sample and container can be minimized by fabricating a container alloy of iron plus, if necessary, inert metal (platinum), then setting the furnace-gas oxygen fugacity value so that the wüstite activity of the container permits the sample to melt at constant bulk composition (Huebner, 1973). The log wüstite activity value during such an experiment cannot be known more accurately than one-half the uncertainty in the log oxygen fugacity value of the furnace atmosphere (because $Fe + 1/2\ O_2$ = "FeO"). In order to assess these uncertainties, direct electrochemical measurements of oxygen fugacity values were compared with values calculated from the mixing ratios of gas components. The resulting discrepancies from two furnaces indicate that the gas mixture cannot always be assumed to equilibrate by the time it reaches the furnace hot spot; thus, knowledge of temperature and gas composition are not necessarily sufficient to calculate the prevailing f_{O_2} and "wüstite" activity.

Apparatus

The experimental apparatus (Fig. 6 of Ross *et al,* 1973), although relatively simple, is divided into four parts for convenience of discussion. A gas-mixing train (1) supplies a stably proportioned gas mixture to a vertical (quenching) furnace (2). An electrochemical cell (3) that is specific for oxygen is placed within the furnace. Two electrical measurement circuits (4) permit continuous recording of temperature and oxygen fugacity.

(1) The gas train is exceedingly simple. Compressed CO_2 and either H_2 or CO are reduced to 5 psi with conventional single-stage flow regulators, then further reduced to about 1 psi (relative) with low flow rate regulators. Gas-flow rates are individually controlled with metering valves or capillary tubes. The gases are mixed in a tube 200 cm long and 2 cm in diameter, filled with ceramic chips and glass wool. Floating ball flow-meters, calibrated for air, indicate the flow rate of the mixed gases. With this gas train, the measured flow rate of the mixed gas will vary less than 3 percent and the f_{O_2} less than ±0.1 log atm unit over a 30-day period.

For calibration experiments, a mechanical gas proportioner is inserted between the metering valves and the flow meter. Each gas is displaced by pistons connected by gears to a single motor, ensuring a constant displacement ratio. Gas bubblers (the bleeder tubes of Darken and Gurry, 1945) filled with dibutyl phthalate keep the input gas pressure ratio at 1.000 ± 0.001. Gas mixing ratios are believed to be accurate to within 1 percent.

(2) A conventional vertically mounted tubular furnace 30.5 cm long heats the alumina muffle tube (1.6 cm I.D. × 2.2 cm O.D.) that carries the gas through the furnace. The 30-cm long helical platinum winding has 4.7 turns per centimeter over its top and bottom 7

[1] Approved for the Director, 2/26/74.

cm, and 3.9 turns per centimeter over its middle to give an even hot spot. The power controller maintains temperature constant within the precision of the temperature-measurement circuit, ±1°C.

(3) The electrochemical oxygen cell (Fig. 1) consists of ZrO_2 doped with 15 wt percent CaO (see Sato, 1971). The ceramic forms a 0.64-cm tube open at one end only. Perforated platinum metal electrodes, crimped to the cell, contact the inner and outer sides of the tube for 0.6 cm at the closed end and serve solely to connect the cell to the measuring circuit. A $Pt\text{-}Pt_{90}Rh_{10}$ thermocouple is positioned within the tip of the cell by means of a 0.32 cm four-bore alumina tube which insulates the thermocouple leads from each other and from the inner electrode lead. Oxygen gas flows at rates of about 0.5 cm^3 $minute^{-1}$ between the inner alumina and outer zirconia tubes to the end of the cell, then exhausts through the fourth bore of the alumina tube. Oxygen serves not only as the reference gas (at unit fugacity) of the cell

$$O_2,\ 1\ atm\ |(Zr,\ Ca)\ O_2|\ O_2,\ \text{furnace atm}$$

but also separates the thermocouple from hydrogen-rich furnace gas (see comments by Caldwell, 1962, p. 5).

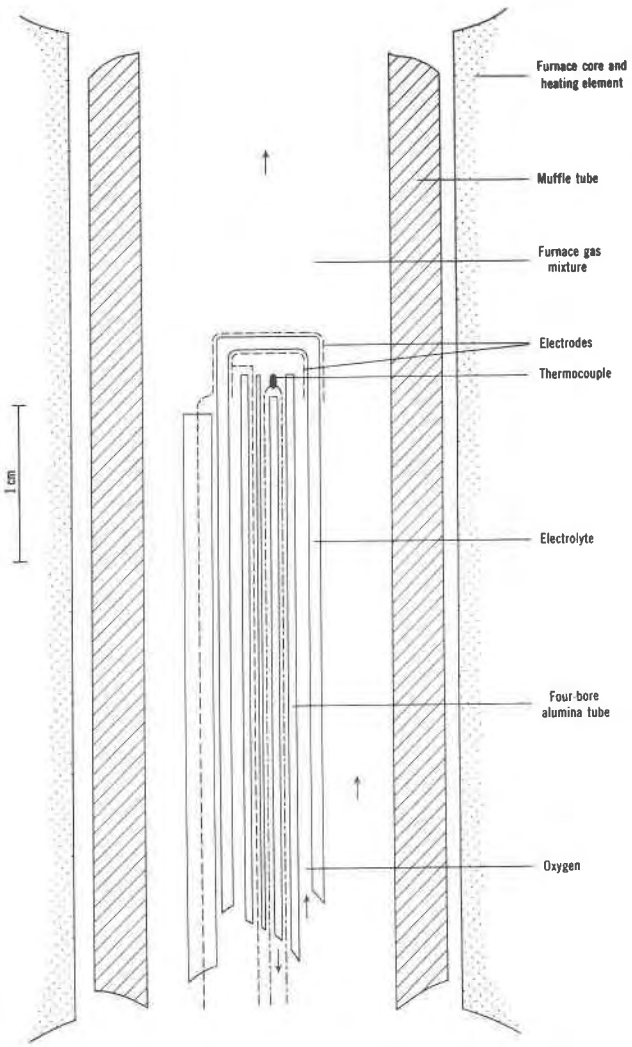

FIG. 1. Vertical section through center of furnace showing the oxygen fugacity and temperature sensors. Oxygen exits through the fourth bore (not shown) of the central alumina tube. Dashed lines are platinum electrodes and their leads; dot-dash lines are the thermocouple leads. Arrows indicate directions of gas flow.

(4) A two-channel strip chart recorder continuously records both thermocouple and cell EMF. The thermocouple is connected in series with a cold junction (ice bath) and one channel of the recorder. The oxygen cell electrodes are connected to the second recorder channel through an electrometer used as an impedance matching device. Each measuring circuit is calibrated against a known EMF source so that measured voltages were accurate to within 0.1 percent of the actual value.

In the experiment described here, the thermocouple temperature, as read on the strip chart, had to be raised by 8°C on the basis of the observed melting points of gold (assumed to be 1064.4°C, IPTS 1968) and NaCl (800.6°C; Robie and Waldbaum, 1968). This 8°C correction is characteristic for all thermocouples made from the same spools of wire. The correction does not change with the thermocouple's length of service at the temperature of interest, <1300°C.

Oxygen fugacity values were calculated using the Nernst relationship

$$\ln f_{O_2}(\text{furnace gas}) - \ln f_{O_2}(\text{reference}) = n \cdot F \cdot \text{EMF}/R \cdot T$$

which for the cell in question reduces to

$$\log f_{O_2}\ (\text{furnace gas}) = (20160)(\text{EMF})(T^{-1})$$

where EMF is in volts, T in degrees Kelvin, and f_{O_2} in log atm units.

Position of Sensors

The thermocouple was firmly positioned within the tip of the cell where it could closely monitor the temperature of the cell. The cell assembly was in turn fixed within the (gas-flow) muffle tube. The hot spot was profiled by incrementally raising or lowering the muffle tube + cell + thermocouple assembly through the furnace. Because the position of the separate ther-

mocouple for the power controller was fixed relative to the winding, the temperature of the furnance winding did not deviate from measurement to measurement.

Typical hot-spot profiles are shown in Figures 2a and 2c. The uniform temperature of ±1 to 2°C over 2 cm is probably about the best to be expected from a singly wound furnace. At all combinations of temperature and gas-flow rate, the hot spots were found to be approximately symmetrical. The position of the hot spot changed little with temperature (<0.5 cm with a 200°C increase) and migrated downstream only slightly when the gas-flow rate increased.

Measured oxygen fugacity values did not always vary symmetrically about the hot spot. This asymmetry, the causes of which will be discussed later, was particularly evident for H_2-CO_2 mixtures (Fig. 2c); as the cell was raised in the direction of the furnace gas flow, the measured oxygen fugacity increased steadily. Adjustment of power to the furnace to maintain a constant measured cell temperature resulted in the same pattern. Clearly these variations in oxygen fugacity are dependent on the position of the sensor, not on temperature. For accurate f_{O_2} control, positioning of a sample, with or without an electrochemical cell, must take cognizance of the variation of f_{O_2} as well as temperature with the position in the furnace.

Under some conditions, particularly high temperatures, mixtures of CO and CO_2 showed an approximately symmetrical variation of oxygen fugacity with temperature as the hot zone of the furnace was profiled with the sensors. The example in Figure 2d, selected because it shows a very small yet smooth variation of f_{O_2} with a small change in temperature, demonstrates the inherent precision in electrochemical oxygen fugacity measurements.

Comparison of Measured and Calculated Oxygen Fugacity Values

Many combinations of sensor position, gas-mixing ratio, and flow rate were examined for both CO_2/H_2 and CO_2/CO gas mixtures. Sensor position, bulk gas composition, and flow rate (at furnace entrance) were maintained constant while temperature was varied between 1250°-1300°C and a much lower temperature (900°-1025°). Results were plotted as a function of temperature and $\Delta\log f_{O_2}$ units where $\Delta\log f_{O_2}$ = (measured $\log f_{O_2}$) − (calculated $\log f_{O_2}$). Calculated $\log f_{O_2}$ values were obtained by interpolating between values calculated by Deines *et al* (1974) from thermochemical data in JANAF Tables (Stull and Prophet, 1971).

Experimental values of $\Delta\log f_{O_2}$ are too large to be due to experimental error in measurement. For instance, at 1054°C, with a gas mixture consisting of

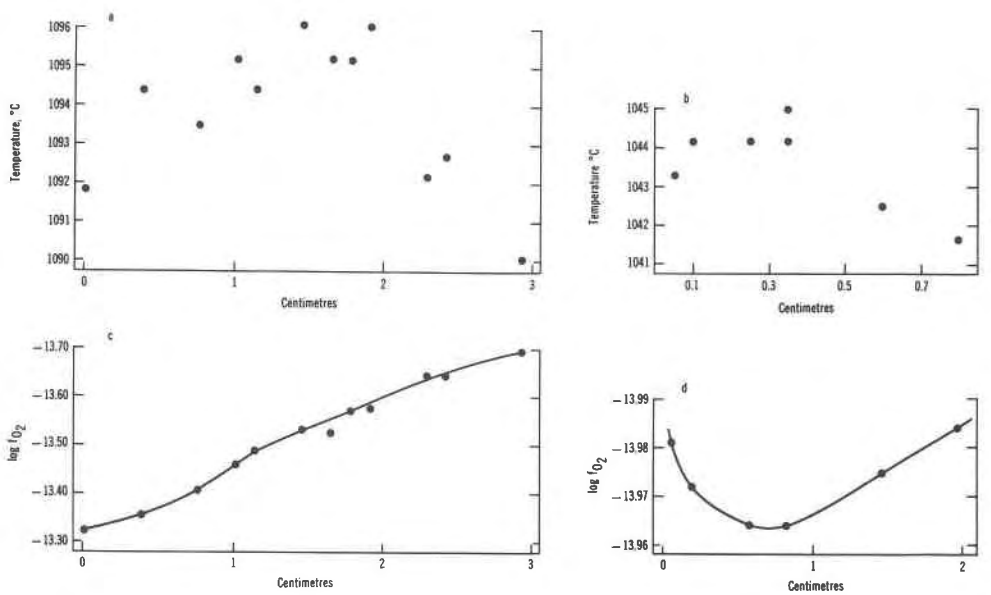

FIG. 2. Temperature and oxygen-fugacity variations across the furnace hot zone. The direction of gas flow is to the left. Figures 2a, 2c: 35.7 percent CO_2 and 64.3 percent H_2; 0.52 cm^3sec^{-1} gas entering furnace; oxygen-fugacity variation asymmetric. Figures 2b, 2d: 33.3 percent CO_2 and 66.7 percent CO; 0.95 cm^3sec^{-1} gas entering furnace; oxygen-fugacity variation symmetric.

35.7 percent CO_2 and 64.3 percent H_2, the observed Δlog atm f_{O_2} value of -0.28 would require that the measured temperature be in error by $+18°C$, that the gas mixture really consists of 29.5 percent CO_2, or that the cell EMF be in error by 18 mV (0.925 V calc versus 0.9435 V obs). Experimental uncertainties, particularly systematic uncertainties, are too small to give rise to the observed discrepancies in oxygen fugacity values.

Impurities in the gases cannot be the cause of the discrepancies. Several tanks of each gas (bone dry and welding grades of carbon dioxide, C.P. carbon monoxide, high purity hydrogen) were acquired over periods ranging from several months to 4 years. The consistent results obtained using a variety of gas tanks eliminate the possibility of random variations in gas purity.

Impurities introduced systematically into the gas tanks or gas train cannot account for the observed log f_{O_2} values. Preferential leakage of a gas species into the gas train should affect the f_{O_2} values of gases with a large value of the mixing ratio (and thus small buffering capacity) to a greater extent than gases with a mixing ratio close to unity (and with greater buffering capacity). The observed pattern of change in Δlog f_{O_2} with temperature did not change with mixing ratio. Furthermore, it is inconceivable that an inert component could be a dilutant systematically included with the tanked gases in such proportion that the mixing ratio of an equally proportioned mixture would change by the required amount—a factor greater than two. Similar reasoning eliminates loss of one of the proportioned gas species as an explanation for the discrepancies. Leakage of oxygen into the system would cause anomalously oxidizing conditions, whereas the approach to equilibrium is from more reducing conditions.

Finally, the presence in an initially proportioned gas mixture of additional gas species from the system C–H–O will have only a small effect on the measured f_{O_2} values. For instance, addition of H_2O to the CO_2 used for a CO_2/CO mixture will not greatly affect the experimental results. This situation arises because of the great similarity of the T-f_{O_2}-mixing ratio relations for CO_2-H_2, CO_2-CO, and H_2O-H_2 mixtures in the range of interest here (compare Figs. 11, 15, and 34 of Muan and Osborn, 1965).

Calibration measurements could not be made below 940°C because the cell EMF fluctuated cyclically. Such oscillations correspond to oscillations in the flow rate measured by the flow meter and are due to incremental additions of gas by the pistons in the gas proportioner. A ballast bottle inserted between the pump and furnace minimized but did not eliminate these oscillations. Such changes in flow rate caused oscillations in the degree of equilibration of the furnace gas (see discussion of results) with resultant cell EMF variations of several millivolts. During the part of the cycle in which gas flowed most quickly, the value of Δlog atm f_{O_2} was most negative.

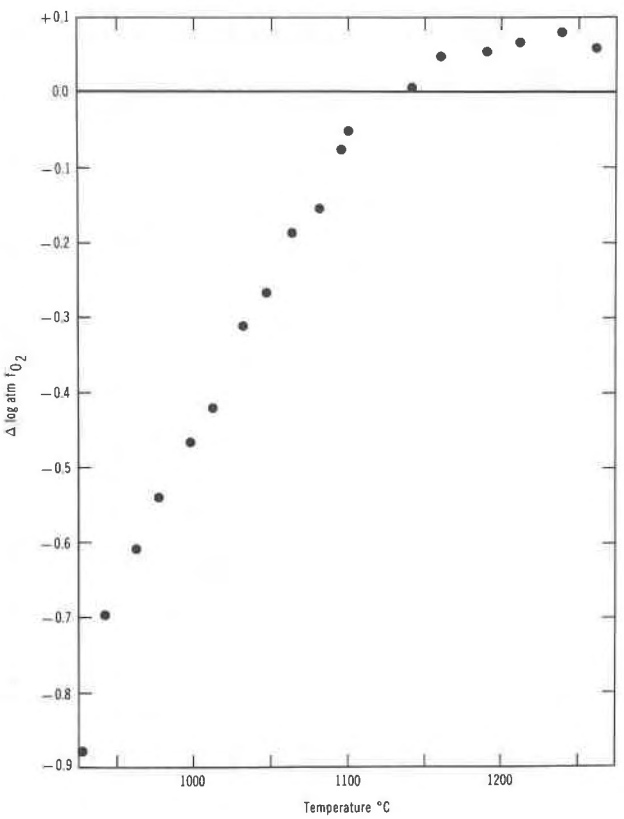

FIG. 3. Variation of Δlog atm f_{O_2} (see text) with temperature for a gas mixture consisting of 35.7 percent CO_2 and 64.3 percent H_2 entering the furnace at 0.52 cm sec^{-1}.

H_2-CO_2 Mixtures

At low temperatures, measured oxygen fugacity values are more reducing (negative Δlog f_{O_2}) than the calculated oxygen fugacities (Fig. 3). As temperature increases, measured f_{O_2} increases relative to calculated f_{O_2}. In all cases, the curve of Δlog f_{O_2} versus T flattens (becomes independent of temperature) at a positive value of Δlog f_{O_2}. This "equilibrium" value of Δlog f_{O_2} appears to depend upon such factors as flow rate and sensor position and varies from $+0.02$ to $+0.13$ log atm units f_{O_2}.

Decreasing the gas-flow rate has a consistent but

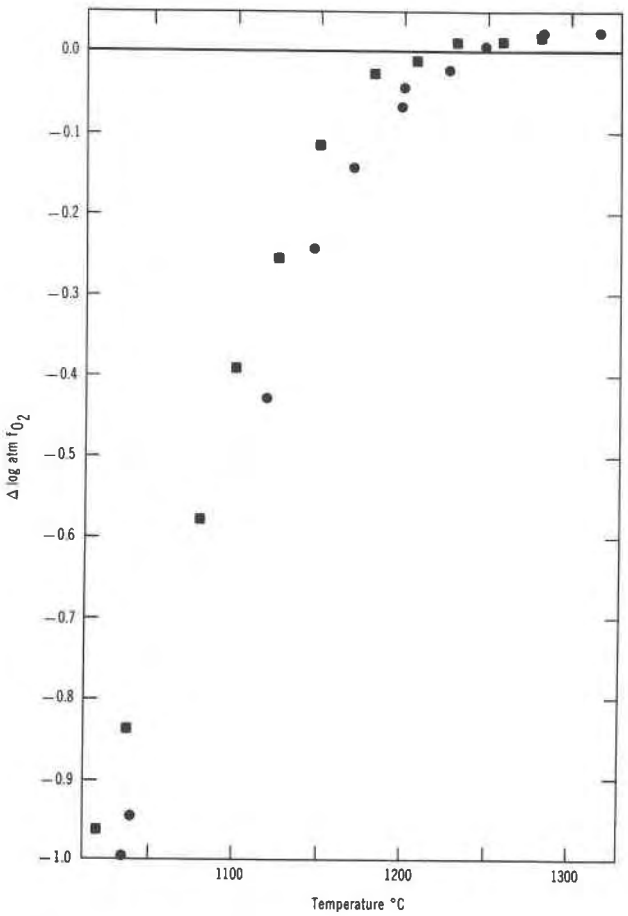

FIG. 4. Change in Δlog atm f_{O_2} with flow rate. Gas mixture consisting of 35.7 percent CO_2 and 64.3 percent H_2. Gas mixture entered furnace at 0.96 cm sec^{-1} (circles) and 0.52 cm sec^{-1} (squares). Sensors were moved 0.5 cm between series of measurements to compensate for shift of hot spot with flow rate.

small effect on the results of an experiment (Fig. 4). Changing the gas-flow rate from 96 to 52 $cm^3 min^{-1}$ (air equivalents) at room temperature has a net effect on Δlog f_{O_2} equivalent to lowering temperature by 25°C. (Assuming a temperature of 1100°C, this change in flow rate corresponds to decreasing the linear flow rate from 4.4 to 2.4 cm sec^{-1} past the outer side of the electrode of the oxygen probe.) If the electrochemical sensor is repositioned to compensate for the shift of hot-spot position with flow rate (0.5 cm in Fig. 3), the "equilibrium" value of log f_{O_2} does not change with flow rate.

The position of the oxygen fugacity sensor relative to the hot spot appears to be a more important factor than variations in flow rate (Fig. 5). Movement of the sensor 1.1 cm in a downstream direction (sensor raised 1.1 cm in furnace) uniformly increases the Δlog f_{O_2} by about 0.1 log atm unit. Particularly important is the fact that the high temperature or equilibrium Δlog f_{O_2} value is also increased.

Change in the gas-mixture ratio changes details of the Δlog f_{O_2} *vs* temperature plot but does not alter the general pattern whereby Δlog f_{O_2} becomes increasingly negative with decreasing temperature. Equilibration problems are not confined to hydrogen-rich mixtures but are also shown by a mixture with 96.2 percent CO_2 (Fig. 6). With this CO_2-rich mixture, the cell EMF oscillated with the flow rate at temperatures below 1100°C, suggesting great disequilibrium within the gas stream. At temperatures less than 1089°C, Δlog f_{O_2} probably becomes strongly negative.

CO_2-CO Mixtures

The CO_2-CO mixtures give results that are similar to the CO_2-H_2 mixtures (Figs. 7-9). When temperature increases, the CO_2-CO mixtures become less reducing relative to calculated f_{O_2} values. The

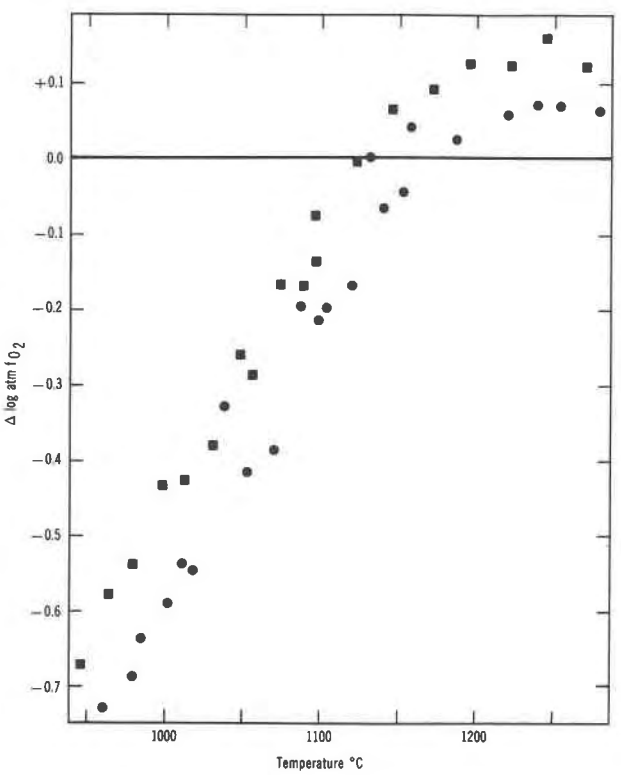

FIG. 5. Change in Δlog atm f_{O_2} with position of sensor relative to hot spot. Gas mixture consisting of 35.7 percent CO_2 and 64.3 percent H_2, entering the furnace at 0.95 cm sec^{-1}. Circles are measurements with the cell positioned at the hot spot; squares are measurements 1.1 cm above (and downstream from) the hot spot.

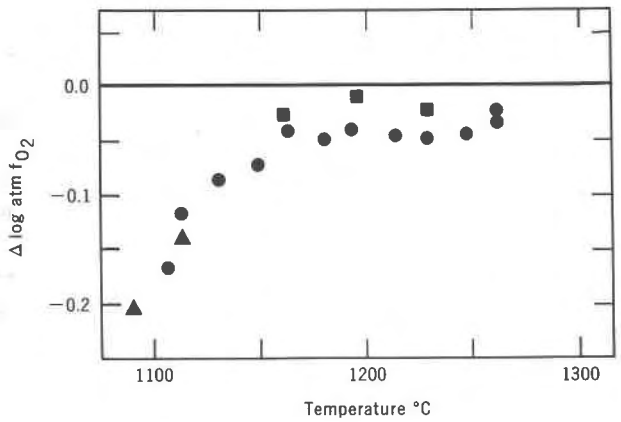

FIG. 6. Variation of Δlog atm f_{O_2} with temperature for a gas mixture consisting of 96.2 percent CO_2 and 3.8 percent hydrogen, entering the furnace at 0.94 cm sec^{-1}. Different symbols represent different series of measurements.

Δlog f_{O_2} versus T curve is flat (Δ independent of T) at 1200°C. The equilibrium Δlog f_{O_2} value is +0.1 to +0.23 log atm units, larger than for H_2-CO_2 mixtures. When temperature decreases, Δlog f_{O_2} does not decrease as rapidly as with H_2-CO_2 mixtures, so even at 1000°C, Δlog f_{O_2} is between −0.3 and +0.04 log atm units.

Changes in gas-flow rate produce only minor changes in logf_{O_2}; if the flow rate is divided by two, the Δlog f_{O_2} versus T curve shifts 15°C toward lower temperatures (Figs. 7,8). If the oxygen fugacity sensor position is moved in a downstream direction 0.9 cm, Δlog f_{O_2} is raised slightly (Figs. 7,9). If the gas composition is changed from 33.3 percent CO_2 to 92.9 percent CO_2, Δlog f_{O_2} is effectively decreased by 0.1 log atm unit (Figs. 7-9).

During two sets of measurements, Δlog f_{O_2} *decreased* with increasing temperature to an otherwise normal value of Δlog f_{O_2}, +0.16 log atm units at ~1100°C. This unusual behavior was not predictable and emphasizes the importance of using an oxygen fugacity sensor to measure f_{O_2} within the furnace.

Carbon sometimes precipitates from CO_2-CO gas mixtures onto the muffle and electrolyte tubes at the very bottom of the furnace, 14 to 16.5 cm below the tip of the oxygen sensor. At low temperatures, the CO_2-CO mixtures are metastable with respect to graphite + gas. On heating, the CO_2-CO mixtures can approach equilibrium by precipitating carbon. When temperature continues to increase, graphite is no longer stable, and thus carbon does not precipitate near the furnace hot zone. Loss of carbon from the gas phase increases the proportion of CO_2 in the mixture (makes a more oxidizing gas mixture) and provides possible explanations for the relatively large values of Δlog atm f_{O_2} found for the CO_2-CO mixtures at high temperature, and the decreases in Δlog f_{O_2} with temperature observed in two experiments.

Cause of the Discrepancies

Two forms of apparent chemical disequilibrium are possible as a gas mixture flows through a furnace. In the first case, the bulk composition of the gas is constant throughout the furnace; the disequilibrium is a kinetic problem, the gas not having enough time to react to equilibrium before its oxygen fugacity is measured. Disequilibrium due to kinetic factors should be lessened by either raising the furnace temperature or decreasing the flow rate. Both of these effects are observed in the reported series of measurements. The observed discrepancies are probably kinetic in origin.

A second form of disequilibrium arises when a gas mixture is placed in a thermal gradient such as that existing in a quenching furnace (*i.e.*, de Groot, 1951, p. 111-123). For CO_2-H_2 mixtures to at least 490°C, CO_2 tends to diffuse to relatively cooler parts of the furnace, whereas H_2 concentrates at the hot spot (Ibbs, 1925; Elliott and Masson, 1925). Apparent disequilibrium due to thermal diffusion can be distinguished from true disequilibrium of kinetic origin. Thermal-diffusion partitioning tends to increase as flow rate decreases (see Darken and Gurry, 1945), whereas kinetic disequilibrium decreases as flow rate decreases. Thermal-diffusion partitioning increases

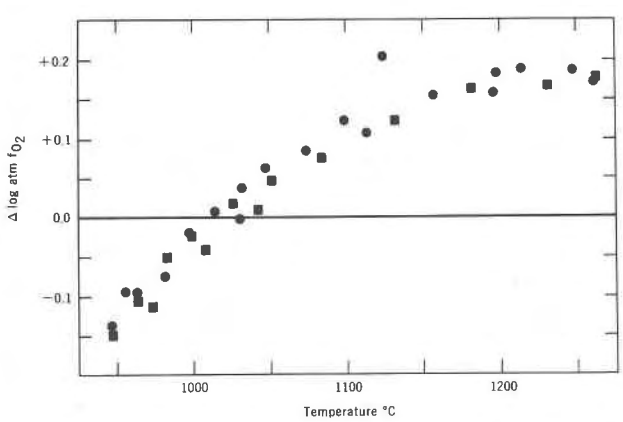

FIG. 7. Variation of Δlog atm f_{O_2} with temperature for a gas mixture consisting of 33.3 percent CO_2 and 66.7 percent CO. Gas mixture entered the furnace at 0.95 cm sec^{-1} (circles) and 0.34 cm sec^{-1} (squares). Sensor positioned at midpoint of hot spot.

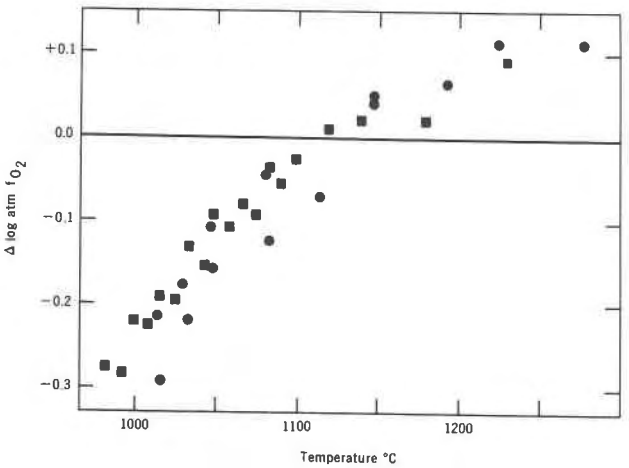

FIG. 8. Variation of Δlog atm f_{O_2} with temperature for a gas mixture consisting of 92.9 percent CO_2 and 7.1 percent CO. Gas mixture entered furnace at 0.96 cm sec^{-1} (circles) and ~0.4 cm sec^{-1} (squares). Sensor positioned as for Figure 7.

as furnace temperature increases (thus steepening the temperature gradient), whereas kinetic disequilibrium decreases as temperature increases. The observed discrepancies reported here cannot be explained by thermal diffusion.

Practical Consideration

The present results suggest that uncertainties involved in experiments utilizing gas-mixing furnaces may be greater than heretofore realized. Precise work requires that the oxygen fugacity gradient, as well as the temperature gradient, be determined. The best position of the sample (within the furnace) may not be at the hot spot. Over much of the temperature range of interest to geologists, the uncertainty in furnace oxygen fugacity can be decreased by moving the sample off the hot-spot plateau in the downstream direction, but at the expense of increasing the uncertainty in the temperature measurement.

The use of an electrochemical sensor to measure the oxygen fugacity in the vicinity of a sample not only decreases the uncertainty of the oxygen fugacity value, but greatly simplifies determination of an oxygen fugacity gradient (compare with the method of Darken and Gurry, 1945). However, because gradients exist even when an oxygen fugacity sensor is present, the oxygen probe must be used with care. Gradients of 0.1 to 0.2 log atm units f_{O_2} over 1 to 2 cm are not uncommon and can lead to relatively great uncertainties in the thermodynamic activity of a component: for the reaction Fe + 1/2 O_2 = FeO, ±0.15 log atm unit in f_{O_2} leads to ±0.075 log units aFeO, or ±19 percent systematic uncertainty in wüstite activity because of the oxygen fugacity gradient alone!

The overall uncertainties reported in this work are greater than the uncertainties suggested by Huebner and Sato (1970) for an oxygen fugacity sensor configuration in which the sample is contained within the sensor (thus minimizing the thermal gradient and isolating the sample from the furnace gas). For the present case, in which the sensor monitors furnace gas f_{O_2}, the precision of oxygen fugacity measurement appears to be approximately ±0.02 log atm units. An uncertainty of ±3°C contributes about ±0.05 log atm units to the uncertainty in oxygen fugacity. Oxygen fugacity gradients within the hot spot commonly lead to systematic uncertainties of 0.1 to 0.2 log atm units. If no oxygen probe is used, there is no random error of measurement, but uncertainties in the thermochemical data from which the f_{O_2} must be calculated, and in degree of equilibration, become important and may give systematic errors of 0.1 log unit and >0.1 log unit, respectively.

The following are guidelines to gas-flow furnace experimentation conducted in this laboratory:

(1) Use an oxygen probe to monitor furnace oxygen fugacity.
(2) At 1000°C or less, great uncertainties in f_{O_2} values exist, even with an oxygen probe.
(3) Position the sample on the downstream side of the hot-spot plateau.
(4) If an oxygen probe was not placed in a furnace and the gas mixtures did not equilibrate, previously reported experiments made at

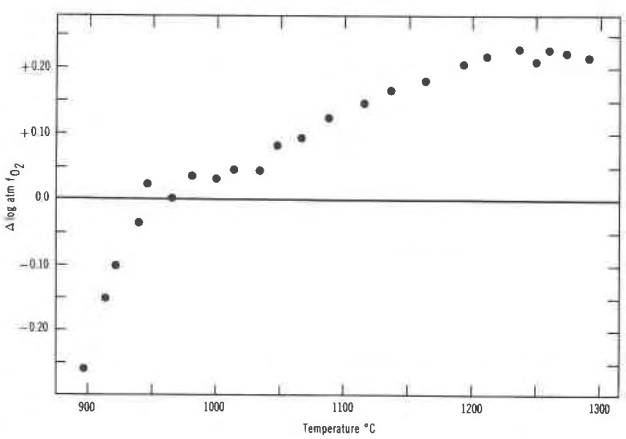

FIG. 9. Variation of Δlog atm f_{O_2} with temperature for a gas mixture consisting of 27.3 percent CO_2 and 72.7 percent CO. Flow rate ~0.9 cm sec^{-1}. Sensor moved 0.9 cm downstream from center of hot spot.

TABLE 1. Experiments Delineating the Iron-Wüstite Equilibrium at 1 Atm

T°C	EMF,V	f_{O_2} Log atm	Time	Stable phase	Calc† log f_{O_2}
1352	0.827	-10.26	2 hrs	I	-10.18
1352	0.819	-10.16	1.7	W	-10.18
1300	0.837	-10.73	1.8	I	-10.73
1300	0.830	-10.63	1.5	W	-10.73
1241	0.854	-11.37	2.3	I	-11.40
1241	0.849	-11.30	3	W	-11.40
1168	0.880	-12.31	3	I	-12.31
1167	0.878	-12.29	2	I	-12.33
1168	0.874	-12.23	2	W	-12.31
1167	0.872	-12.21	16.5	W	-12.33
1126	0.922	-13.28	2.7	I	-12.88
1124	0.916	-13.21	1.5	I,W	-12.91
1125	0.912	-13.15	3.2	W	-12.89
1084	0.931	-13.82	2.3	I	-13.48
1084	0.928	-13.78	1.8	W	-13.48
1084	0.916	-13.60	2.7	W	-13.48
1042	0.949	-14.55	7.5	I	-14.12
1047	0.947	-14.46	3.5	I**	-14.04
1030	0.940	-14.54	7.5	W	-14.31
1047	0.939	-14.34	3	W	-14.04

*I, iron stable; W, wüstite stable
**very little reaction to form iron; much wüstite remains
†from Eugster and Wones (1962) equation

temperatures below 1100-1200°C might reflect f_{O_2} values lower than was reported.

(5) Keep the sample small and place the sample as close to the sensor as possible. Avoid contacts which might contaminate the sensor electrode.

Redetermination of the Iron-Wüstite Equilibrium

The iron-wüstite equilibrium was redetermined using $CO_2 + H_2$ gas mixtures and a furnace configuration similar to that described previously. The experimental charge, an open iron-foil packet containing wüstite, was suspended about 2.4 mm above the outer electrode of the oxygen cell, on the downstream side of the thermal plateau. Gases were not pumped with a mechanical proportioner; rather, the desired furnace cell EMF was provided by leaking the CO_2 and H_2 through metering valves. The gas mixture was supplied to the furnace continuously. At each temperature, the Fe-$Fe_{1-x}O$ equilibrium was narrowly bracketed. Results are listed in Table 1 and plotted in Figure 10.

At 1160-1350°C, closely bracketed oxygen-cell measurements yield f_{O_2} values 0.03-0.07 log atm units above the famous log f_{O_2} *vs* T curve of Eugster and Wones (1962) and Darken and Gurry (1945). The agreement is excellent. The small systematic discrepancy is not significant—it could come about due to uncertainties in temperature measurement and distribution. However, at 1040-1125°C, reversed runs suggest log f_{O_2} values 0.2 units more reducing than the reference curve. The discrepancy is significant and may best be explained by an f_{O_2} gradient in the furnace. The furnace gas in the vicinity of the sensor, which is upstream from the sample, has a lower oxygen fugacity than the furnace gas in the vicinity of the sample. Because the sample f_{O_2} varies greatly with position in the furnace, the discrepancy at low temperature is erratic. Even small changes in sample position from run to run produce measurable oxygen fugacity variations.

Thermochemical Data for Gases

All measured deviations from equilibrium oxygen fugacity are referred to log f_{O_2} values calculated from thermochemical data contained in the JANAF Tables. At high temperatures, the measured equilibrium or steady-state oxygen fugacity value is consistently more positive than the calculated f_{O_2} values by about 0.06 log atm units (CO_2-H_2) to about 0.15 such units (CO_2-CO). Such a discrepancy is larger than that attributable to an uncertainty in temperature (a deviation of 0.15 log atm unit for a mixture of 33 percent CO_2, 67 percent CO, requires an error of 10°C). A more probable explanation is a minor error in the thermochemical data. Deines *et al* (1974) have compared the JANAF data with other earlier internally consistent sets of data for C–O–H

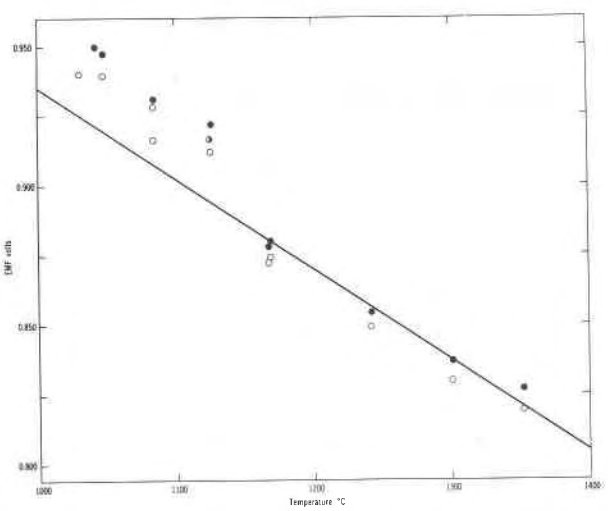

FIG. 10. Experiments delimiting the iron-wüstite equilibrium. Open circles, wüstite stable. Closed circles, iron stable. Straight line—the iron-wüstite equilibrium calculated from the equation in Eugster and Wones (1962).

system gases. In support of the present measurements, the JANAF data yields f_{O_2} values that are 0.04 − 0.20 log atm units more negative than the other sets of data. It should be emphasized, though, that application of $\Delta \log f_{O_2}$ values to a redetermination of the thermochemical data for C–H–O gases requires a new set of careful experiments using analyzed gases.

Acknowledgment

I am grateful to Drs. Peter Deines and Gene Ulmer for providing me with copies of their T-X-log f_{o_2} tables and figures before formal publication. I want to thank Miss Mary Woodruff of the U.S. Geological Survey who checked numerous calculations and assisted in the manuscript preparation.

References

CALDWELL, F. R. (1962) Thermocouple materials. *U.S. Natl Bur. Stand. Monogr.* **40,** 43 p.

DARKEN, L. S., AND R. W. GURRY (1945) The system iron-oxygen. 1. The wüstite field and related equilibria. *J. Am. Chem. Soc.* **67,** 1398–1412.

DEINES, P., R. H. NAFZIGER, G. C. ULMER, AND E. WOERMANN (1974) T-f_{o_2} tables for selected gas mixtures in the C–H–O system at one atmosphere total pressure. *Bull. Earth Mineral Sci. Exp. Stn,* **88,** 1–129.

DE GROOT, S. R. (1951) *Thermodynamics of Irreversible Processes.* Amsterdam: North Holland Publishing Co., 242 p.

ELLIOTT, G. A., AND IRVINE MASSON (1925) Thermal separation in gaseous mixtures. *Roy. Soc. London Proc.* **A108,** 378–385.

EUGSTER, HANS P., AND DAVID R. WONES (1962) Stability relations of the ferruginous biotite, annite. *J. Petrol.* **3,** 82–125.

HUEBNER, J. S. (1973) Experimental control of wüstite activity and mole fraction. *Geol. Soc. Am. Abstr.* Programs, **5,** 676–677.

———, AND MOTOAKI SATO (1970) The oxygen fugacity-temperature relationships of manganese oxide and nickel oxide buffers. *Am. Mineral.* **55,** 934–952.

IBBS, T. L. (1924) Thermal diffusion measurements. *Roy. Soc. London Proc.* **107A,** 470–486.

MUAN, ARNULF, AND E. F. OSBORN (1965) Phase equilibria among oxides in steelmaking. Reading, Pennsylvania, Addison Wesley Publishing Co., Inc., 236 p.

ROBIE, R. A., AND DAVID R. WALDBAUM (1968) Thermodynamic properties of minerals and related substances at 298.15°K (25.0°C) and one atmosphere (1.013 bars) pressure and at higher temperatures. *U.S. Geol. Surv. Bull.* **1259,** 256 p.

ROSS, MALCOLM, J. S. HUEBNER, AND ERIC DOWTY (1973) Delineation of the one atmosphere augite-pigeonite miscibility gap for pyroxenes from lunar basalt 12021. *Am. Mineral.* **58,** 619–635.

SATO, MOTOAKI (1971) Electrochemical measurements and control of oxygen fugacity and other gaseous fugacities with solid electrolyte sensors. In, *Research Techniques for High Pressure and High Temperature,* Gene C. Ulmer, Ed. New York, Springer Verlag, p. 43–99.

STULL, D. R., AND H. PROPHET (1971) JANAF Thermochemical Tables, Second Edition. *U.S. Natl Bur. Stand, Ref. Data Ser.* **37,** 1141 p.

Manuscript received, December 16, 1974; accepted for publication, May 5, 1975.